

Self-Assembled Monolayers and Multilayers of Conjugated Thiols, α,ω -Dithiols, and Thioacetyl-Containing Adsorbates. Understanding Attachments between Potential Molecular Wires and Gold Surfaces

James M. Tour,^{*,†,‡} LeRoy Jones II,[‡] Darren L. Pearson,[‡] Jaydeep J. S. Lamba,[‡] Timothy P. Burgin,[‡] George M. Whitesides,^{*,§} David L. Allara,^{*,⊥} Atul N. Parikh,[⊥] and Sundar V. Atre[⊥]

Contribution from the Department of Chemistry and Biochemistry, University of South Carolina, Columbia, South Carolina 29208, Department of Chemistry, Harvard University, Cambridge, Massachusetts 02138, and Department of Chemistry, The Pennsylvania State University, University Park, Pennsylvania 16802

Received February 2, 1995[⊗]

Abstract: This paper describes studies of the formation of self-assembled monolayers (SAMs) and multilayers on gold surfaces of rigid-rod conjugated oligomers that have thiol, α,ω -dithiol, thioacetyl, or α,ω -dithioacetyl end groups. The SAMs were analyzed using ellipsometry, X-ray photoelectron spectroscopy (XPS), and infrared external reflectance spectroscopy. The thiol moieties usually dominate adsorption on the gold sites; interactions with the conjugated π -systems are weaker. Rigid rod α,ω -dithiols form assemblies in which one thiol group binds to the surface while the second thiol moiety projects upward at the exposed surface of the SAM. In situ deprotection of the thiol moieties by deacylation of thioacetyl groups using NH_4OH permits formation of SAMs without having to isolate the oxidatively unstable free thiols. Moreover, direct adsorption, without exogenous base, of the thioacetyl-terminated oligomers can be accomplished to generate gold surface-bound thiolates. However, in the non-base-promoted adsorptions, higher concentrations of the thioacetyl groups, relative to that of thiol groups, are required to achieve monolayer coverage in a given interval. A thiol-terminated phenylene–ethynylene system was shown to have a tilt angle of the long molecular axis of $<20^\circ$ from the normal to the substrate surface. These aromatic α,ω -dithiol-derived monolayers provide the basis for studies leading to the design of molecular wires capable of bridging proximate gold surfaces.

Introduction

Organic compounds have the potential to serve as molecular components of electronic devices.¹ As a prelude to the design of such devices, it is valuable to understand electrical conduction through single or small arrays of conjugated organic molecules that might ultimately serve as molecular wires.² Here we describe studies of self-assembled monolayers³ (SAMs) derived from a series of sulfur-terminated conjugated oligomers. In several of the oligomeric system studies, the conjugated oligomers are α,ω -dithiol substituted; such functionalities are necessary for binding between proximate gold probes in future electronic conduction experiments. Methods are also described for (1) the in situ NH_4OH -promoted deprotection of acetyl-

protected thiols and (2) the non-base-promoted adsorption of thioacetyl-terminated oligomers on gold, to ultimately form surface-bound thiolates. This study establishes the geometry and density of packing of these rigid-rod aromatic oligomers on gold surfaces. The systems studied here (1) are surface-bound via an aromatic thiol unit, thus there is no potentially insulating alkyl fragment between the aromatic moieties and the gold, (2) do not possess long-chain alkyl termini to direct packing, and (3) are well-suited to evaluate the effect of the thiophene sulfur adsorption propensities versus the terminal thiol adsorption.⁴

Results and Discussion

Monothiols. The ellipsometric and X-ray photoelectron spectroscopic (XPS) data for the various compounds studied are presented in Table 1 along with the calculated monolayer

[†] Surface studies conducted while on sabbatical leave at Harvard University.

[‡] University of South Carolina.

[§] Harvard University.

[⊥] The Pennsylvania State University.

[⊗] Abstract published in *Advance ACS Abstracts*, September 1, 1995.

(1) (a) *Molecular Electronics: Science and Technology*; Aviram, A., Ed.; Confer. Proc. No. 262; American Institute of Physics: New York, 1992. (b) *Molecular Electronic Devices II*; Carter, F. L., Ed.; Marcel Dekker: New York, 1987. (c) Miller, J. S. *Adv. Mater.* **1990**, *2*, 378, 495, 601. (d) Waldeck, D. H.; Beratan, D. N. *Science* **1993**, *261*, 576. (e) Tour, J. M.; Wu, R.; Schumm, J. S. *J. Am. Chem. Soc.* **1991**, *113*, 7064.

(2) (a) *Nanostructure Physics and Fabrication*; Reed, M. A., Kirk, W. P., Eds.; Academic Press: New York, 1989. (b) *Nanostructures and Mesoscopic Systems*; Kirk, W. P., Reed, M. A., Eds.; Academic: New York, 1992.

(3) For an overview on SAMs, see: Ulman, A. *An Introduction to Ultrathin Organic Films*; Academic: Boston, 1991.

(4) No clear predictive pattern of molecular structures has previously been established and only a few studies in which structures have been well-characterized are available. Studies involving SAMs of alkyl chain derivatized aromatic thiols on gold show that the long alkyl chains can organize and force the aromatic rings to tilt away from the surface. For example, see: Chang, S.-C.; Chao, I.; Tao, Y.-T. *J. Am. Chem. Soc.* **1994**, *116*, 6792. Evans, S. D.; Urankar, E.; Ulman, A.; Ferris, N. *J. Am. Chem. Soc.* **1991**, *113*, 4121. Studies of purely aromatic thiolate SAMs on gold indicate that the average tilt of the aromatic rings could range from vertical (Sabatani, E.; Cohen-Boulakia, J.; Breuning, M.; Rubenstein, I. *Langmuir* **1993**, *9*, 2974), to partially tilted (Kwan, W. S.; Atanasoska, L.; Miller, L. L. *Langmuir* **1991**, *7*, 1419), to parallel to the surface (Hutchison, J. E.; Postlethwaite, T. A.; Murray, R. W. *Langmuir* **1993**, *9*, 3277).

Table 1. Data of Layered Structures Prepared from Rigid Rod Thiols, α,ω -Dithiols, and Thioacetyl-Containing Substrates^a



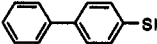
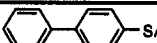
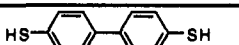
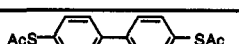
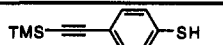

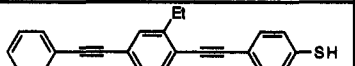
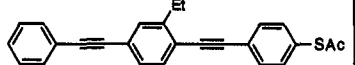
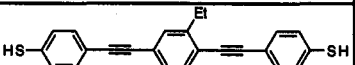
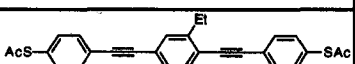
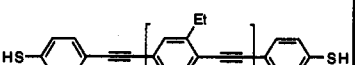
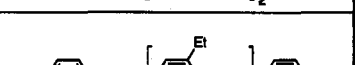

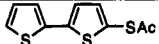
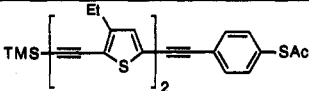
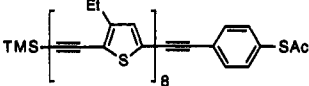
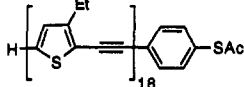
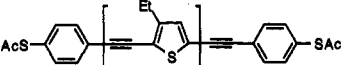
Entry	Compound	Concentration (mM)	Additive ^b	Calc'd SAM Depth (Å) ^c	Found Depth by Ellipsometry (Å) ^d	XPS Data (eV) ^e		
						Au(4f _{7/2}) S(2p _{3/2}) O(1s)	Au(4f _{5/2}) S(2p _{1/2})	C(1s) Si(2p)
1		1.0	----	9.5	14.6 (1 d), 14.5 (3 d)	84 (566) 163 (134) 531 (42)	88 (425) 164 (67)	284 (125) ---
2a		1.0	----	12.1	6.5 (1 d)			
2b	"	41	----	12.1	10.1 (1 d)			
2c	"	1.0	NH ₄ OH	9.5	7.4 (1 d)			
3		1.0	----	12.4	4.9 (1 h), 10.2 (1 d)	84 (678) 162 (32) 531 (13)	88 (509) 163 (16)	284 (91) ---
4a		1.0	----	12.4	6.6 (1 h), 6.9 (1 d)			
4b	"	38	----	12.4	8.9 (1 d)	84 (791) 162 (20) 531 (22)	88 (610) 163 (10)	284 (64) ---
4c	"	1.0	NH ₄ OH	12.4	10.6 (1 d)	84 (708) 162 (27) 531 (33)	88 (531) 163 (13)	284 (101) ---
5		1.0	----	13.6	15.1 (1 d), 17.3 (3 d)	84 (489) 163 (88) 531 (42)	88 (367) 164 (44)	284 (141) ---
6a		0.5	----	16.3	7.8 (1 d)			
6b	"	31	----	16.3	20.5 (1 d)	84 (622) 163 (52) 532 (24)	88 (487) 164 (26)	284 (114) ---
6c	"	0.5	NH ₄ OH	13.6	15.0 (1 d)	84 (723) 163 (50) 531 (26)	88 (570) 164 (25)	284 (105) ---
7		1.0	----	13.2	5.5 (1 h), 11.1 (1 d)	84 (691) 162 (28) 531 (19)	88(519) 163 (14)	284 (70) 100 (72)
8a	 1	1.0	----	13.2	2.2 (1 h), 6.0 (1 d)			
8b	"	36	----	13.2	5.1 (1 d), 14.2 (3 d)	84 (803) 162 (27) 531 (17)	88 (602) 163 (14)	284 (66) 100 (48)
8c	"	1.0	NH ₄ OH	13.2	12.2 (1 d)	84 (644) 162 (32) 530 (18)	88 (484) 163 (16)	284 (69) 101 (36)
9		0.3	----	21.3	13.3 (1 h), 19.0 (1 d)	84 (516) 162 (29) 531 (14)	88 (387) 163 (15)	284 (135) ---
10a	 2	0.3	----	21.3	6.1 (1 h), 8.3 (2 d)			
10b	"	0.3	NH ₄ OH	21.3	18.8 (1 d)	84 (547) 162 (17) 531 (46)	88 (410) 163 (9)	284 (134) ---
11		0.3 ^f	----	22.6	38.4 (1 d), 44.0 (2 d)	84 (181) 163 (69) ---	88 (136) 165 (34)	284 (163) ---
12a		0.1	----	25.2	14.5 (2 d)			
12b	"	0.1	NH ₄ OH	22.6	43.9 (1 d), 53.1 (4 d)			
13		0.1 ^f	----	29.1	51.6 (1 d), 74.0 (2 d)	84 (92) 163 (63) ---	88 (69) 164 (31)	284 (215) ---
14a		0.1	----	31.9	11.7 (1 d), 11.6 (4 d)			
14b	"	0.1	NH ₄ OH	29.1	36.7 (1 d), 58.0 (4 d)			
15		0.5	NEt ₃ ^g	11.6	10.0 (1 d)	84 (700) 163 (84) 532 (19)	88 (525) 164 (42)	284 (83) ---

Table 1 (Continued)

Entry	Compound	Concentration (mM)	Additive ^b	Calc'd SAM Depth (Å) ^c	Found Depth by Ellipsometry (Å) ^d	XPS Data (eV) ^e		
						Au(4f _{7/2}) S(2p _{3/2}) O(1s)	Au(4f _{5/2}) S(2p _{1/2})	C(1s) Si(2p)
16		39	----	11.6	6.4 (1 d), 13.2 (3 d)	84 (723) 163 (54) 531 (19)	88 (543) 164 (28)	284 (82) ---
17a		0.1	----	25.2	7.7 (1 d)			
17b	"	0.1	NH ₄ OH	25.2	21.3 (1 d)	84 (505) 163 (69) 531 (73)	88 (389) 164 (35)	284 (125) --- ^h
18		0.4	NH ₄ OH	63.9	20.5 (1 d), 22.4 (3 d)			
19		0.1	NH ₄ OH	108.3	19.6 (1 d), 28.3 (3 d)			
20a		0.1	----	68.9	23.0 (1 d)			
20b	"	0.1	NH ₄ OH	66.4	32.6 (1 d), 50.8 (4 d)			

^a All adsorption experiments were run without stirring in THF, unless otherwise noted, and they were run on the bench top under an atmosphere of argon. The Au (500 Å) was freshly deposited by electron-beam evaporation on a Ti-primed (20 Å) silicon (100) wafer. ^b In the cases where NH₄OH was added to the reactions, 3–5 μL of NH₄OH (30% aqueous) was added per mg of substrate. Gentle agitation of the vessel for 2 min permitted dissolution of NH₄OH in the THF. ^c The distances were calculated, from an sp-hybridized Au atom to the furthest most proton, by molecular mechanics, for the minimum energy extended forms. Au–S–C bond angles were assumed to be linear.⁴ The Au–S distance was calculated to be 2.36 Å.⁶ ^d The ellipsometric data were obtained using a Rudolph Industries 200E ellipsometer and contain approximately ±5% error. The He–Ne laser (632.8 nm) light was incident at 70° on the sample. Data were taken on 3–4 spots in different regions of a given sample, then averaged. An index of refraction (*n_f*) of 1.55 was assumed for all the film thickness calculations. The values in parentheses correspond to the amount of time that the gold sample was in the solution. ^e The numbers in parentheses are the relative intensities. The XPS data were obtained using a Surface Science SSX-100 XPS using a monochromatic Al Kα source.⁷ The samples were run in random order with the following common parameters: pass energy = 100 eV, spot size = 600 μm, take-off angle⁴⁵ = 35° from the surface plane. The Au(4f_{7/2}) peak was used as a calibration by standardizing to 83.98 eV, the ASTM standard. A 20 eV window was used for all samples and intensity normalization was done between batches by overlapping at least one sample and using the Au(4f_{7/2}) or C(1s) intensities as a calibration point.⁷ Oxidation of the self-assembled layers was noted by the formation of oxidized S(2p) peaks at 167–168 eV and increases in O(1s) content over 5–10 days of storage in air. Therefore, the S(2p) and O(1s) intensities listed here are not useful relative calibration parameters. The background silicon from the wafer gave a broad weak signal at 99 eV that was usually distinguishable from the Si(2p) of the organic.⁷ Adsorption was carried out in CH₂Cl₂. There were solids, presumably oligodisulfides, present throughout the experiment and a small stir bar was placed in the vessel such that it did not hit the gold sample. ^f 6 μL of NEt₃ was added per mg of substrate to liberate the free thiol since the majority of the starting material exists as a dimeric, though not the disulfide, species.⁸ ^h In this case, the Si(2p) of the organic was not easily distinguishable from the background signal.

SAM thicknesses.⁵ Comparison of the XPS intensities from organic-covered gold substrates versus the organic layer thickness measured by ellipsometry confirms the necessary correlation between the data from the XPS and ellipsometry (Figure 1).⁷ In the case of the monothiols, the inference from the data is that several of the oligomers form single monolayers whose thicknesses correspond to the extended, end-to-end distance of

(5) The 1,4-phenyldithiol, 1,4-phenyldithioacetyl, 4-biphenylthiol, 4-biphenylthioacetyl, 4,4'-biphenyldithiol, 4,4'-biphenyldithioacetyl, bithiophenethiol, and bithiophenethioacetyl were prepared by lithium–halogen exchange on the corresponding aryl bromides followed by quenching with sulfur then acetyl chloride or water to generate the thioacetyl compounds or thiols, respectively. For sulfur quench without acylation, see: Jones, E.; Moodie, I. M. *Org. Synth.* **1970**, *50*, 104. For original references to some of these compounds, see: Adams, R.; Ferretti, A. *J. Am. Chem. Soc.* **1959**, *81*, 4939. Kharasch, N.; Swidler, R. *J. Org. Chem.* **1954**, *19*, 1704. Fields, E. K.; Meyerson, S. J. *Org. Chem.* **1969**, *34*, 2475. Klemm, L. H.; Karchesy, J. J. *Heterocycl. Chem.* **1978**, *15*, 281, 561. 1 was prepared from 1-bromo-4-((trimethylsilyl)ethynyl)benzene (Stephens, E. B.; Tour, J. M. *Macromolecules* **1993**, *26*, 2420) following the above thioacetyl-formation protocol. For the preparations of the extended oligomers, see: Schumm, J. S.; Pearson, D. L.; Tour, J. M. *Angew. Chem., Int. Ed. Engl.* **1994**, *33*, 1360. Pearson, D. L.; Schumm, J. S.; Tour, J. M. *Macromolecules* **1994**, *27*, 2348. The arylthioacetyl end groups were affixed to the oligomers via an aryl halide-terminal alkyne cross-coupling, see: Sonogashira, K.; Tohda, Y.; Hagihara, N. *Tetrahedron Lett.* **1975**, 4467.

(6) Modified MM2 force-field, Version 3.7, from CAChe Scientific Inc.

(7) Bain, C. D.; Whitesides, G. M. *J. Phys. Chem.* **1989**, *93*, 1670.

(8) Ponticello, G. S.; Habecker, C. N.; Varga, S. L.; Pitzeneberger, S. M. *J. Org. Chem.* **1989**, *54*, 3223.

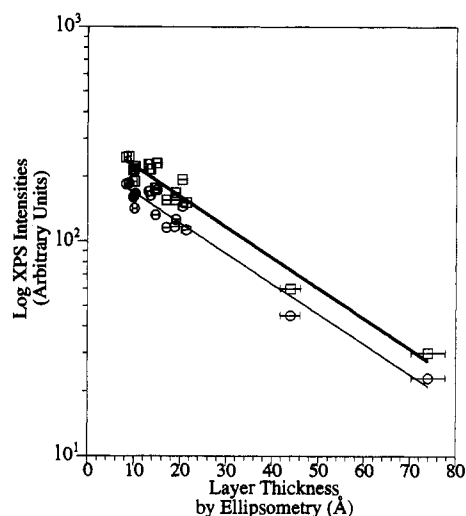


Figure 1. Log of the XPS intensities from organic-covered Au substrates versus the organic layer thickness measured by ellipsometry [Au(4f_{7/2}) (squares) and Au(4f_{5/2}) (circles)]. One scan was used to minimize damage effects over a 15-eV window.⁷ All other parameters were as described in Table 1.

the molecules, suggesting that the organic compounds are nearly normal to the surface (Table 1, entries 3, 7, 9, and 15). The

presence of the aryl groups, with their potential adsorbing π and/or thiophene sulfur centers, seems not to influence the mode of adsorption in several of the systems investigated.⁴ Formation of SAMs from these rigid-rod compounds is slower than with *n*-alkanethiols, the former requiring 1 day to reach a near complete monolayer.

α,ω -Dithiols. Aromatic thiols oxidize readily, and previous work with flexible α,ω -dithiols has suggested that they can form multilayers via disulfide linkages or they can form looped structures where both ends of the molecule bind to the surface.⁹ With these rigid α,ω -dithiols, there was no indication for looped structures wherein both thiol ends were adsorbed to the surface. However, multilayer formation was observed which indicates that one thiol end adsorbed to the surface while the other end projected away from the surface and became available for oxidative S–S coupling (Table 1, entries 1, 5, 11, and 13).^{9,10} Note that these adsorption studies were conducted on the bench top, and though flushing with N₂ was done to reduce oxygen content in the reaction vessels, the systems were not oxygen free. Thus these studies demonstrate the types of adsorptions that could be expected under normal fabrication conditions for electronics.

Acetyl-Protected Monothiols. We have found that acetyl-protected thiols provided an excellent method to alleviate the problems of isolating and using the oxidatively unstable thiols. In the cases where monothiolate-containing systems (ArS) were needed, we could have used disulfides (Ar–SS–Ar) as precursors;³ this strategy, however, is impractical for the α,ω -dithiols, since successive oxidative oligomerization would generate insoluble poly(disulfides). ¹H NMR and ¹³C NMR analysis in THF-*d*₈ showed that **1** (Table 1, entry 8a) could be deacetylated completely within 10 min using aqueous NH₄OH. Other bases such as (*n*-C₃H₇)₂NH or DMAP were far less effective.¹¹ NH₄-OH-promoted removal of the alkynyl-TMS group in **1** was not observed within 72 h. Therefore, in situ deprotection of the monoacetyl-containing systems could be carried out using NH₄-OH to form SAMs (Table 1, entries 4c, 8c, 10b, 17b, 18, and 19). Oligomers up to the 20–25 Å size range (Table 1, entries 10b and 17b) form SAMs efficiently; however, the longer nonlinear oligo(thiophene–ethynylene)s did not proceed to a densely packed SAM (Table 1, entries 18 and 19). In these latter two cases, we cannot exclude the possibility of competitive adsorption between the thiol and thiophene moieties.

The monothioacetyl moiety could even be used, without deprotection by exogenous base, to generate the SAM directly, though higher concentrations of thioacetyl-containing adsorbates, relative to thiols, were required to achieve monolayer coverage (Table 1, entries 4a, 4b, 8a, 8b, 10a, 16, and 17a). We have not determined the mechanism of the adsorption, and though direct adsorption of the thioester to form the gold thiolate is a possibility,¹² hydrolysis of the thioesters, via trace amounts of water or enol forms of the thioesters, is also a plausible reaction course. In the cases of the direct adsorption or base-promoted adsorptions of the thioacetyl-terminated systems, the XPS results confirmed that the SAMs were similar in their composition to the SAMs generated from the free thiols.

Acetyl-Protected α,ω -Dithiols. NH₄OH-promoted deprotection of α,ω -dithioacetyl compounds is a convenient method

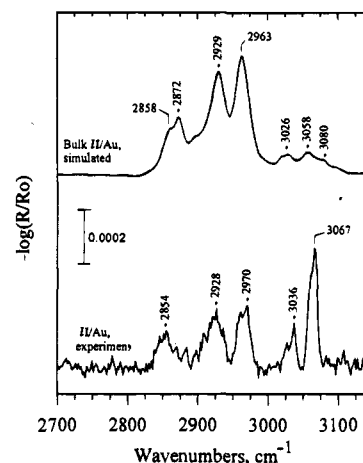


Figure 2. Simulated (top) and experimental (bottom) high wavenumber portion of the FTIR spectrum of **2** after SAM formation on Au. Spectra were collected using an in-house modified Fourier transform spectrometer (FTS-60, Bio-Rad, Cambridge, MA). Incoming *p*-polarized infrared radiation was focused on the sample with an $\sim f/20$ beam impinging at an 85° angle of incidence and the reflected beam was detected using a narrow band MCT detector cooled with liquid nitrogen.¹⁴ The spectra were collected at 2 cm⁻¹ resolution with a mirror velocity corresponding to a data collection rate of 20 kHz. The interferograms were Fourier transformed with triangular apodization and zero-filling. The spectral intensities are reported as reflectivities in absorption units, $-\log(R/R_0)$ where R_0 is the reflectivity of a reference sample prepared by freshly cleaning an evaporated Au substrate using a UV-ozone cleaner (model uvc-100, Boekle Industries, Philadelphia, PA). Optical function spectra of **2** were determined from the normal incidence transmission spectrum of a KBr pellet using a previously published method.¹⁵

to generate the oxidatively unstable dithiols, in situ (Table 1, entries 2c, 6c, 12b, 14b, and 20b). However, deposition with multilayer formation is still problematic when the reactions are conducted in the presence of small amounts of oxygen. Direct adsorption of the α,ω -dithioacetyl compounds appears to be an excellent method for deposition without multilayer formation, though higher concentrations are required (Table 1, entries 2a, 2b, 6a, 6b, 12a, and 14a).^{9,10,13} This direct adsorption method might be particularly well-suited for the deposition of a SAM between proximate gold probes; however, we did not have sufficient quantities of the larger α,ω -dithioacetyl compounds to investigate the efficiency of this process with the longer difunctional oligomers.

Infrared Studies. Infrared external reflectance spectroscopy studies were conducted on SAMs prepared from **2** (deposited using NH₄OH as in Table 1, entry 10b). The results are in agreement with the ellipsometric and XPS data obtained. Figures 2 and 3 show the high- and low-frequency parts, respectively, of the reflection spectrum of the SAM on a gold substrate. Limited experiments also were done with **2** on silver substrates and it was observed that monolayers self-assembled with infrared spectra quite similar to those in Figures 2 and 3. The latter sets of results are part of a more extensive study and will be reported separately.¹⁶ The mode assignments generally were made in analogy with available published assignments for similar structures in pure, bulk phases.¹⁷

(9) Bain, C. D.; Troughton, E. B.; Tao, Y.-T.; Evall, J.; Whitesides, G. M.; Nuzzo, R. G. *J. Am. Chem. Soc.* **1989**, *111*, 321.

(10) (a) Bell, C. M.; Arendt, M. F.; Gomez, L.; Schmehl, R. H.; Mallouk, T. E. *J. Am. Chem. Soc.* **1994**, *116*, 8374. (b) Kim, T.; Crooks, R. M.; Tsen, M.; Sun, L. *J. Am. Chem. Soc.* **1995**, *117*, 3963.

(11) We avoided the use of bases containing metal cations such as NaOH since metal cations are troublesome impurities in fabrication of silicon-based electronic devices.

(12) It was recently reported that a dialkyl sulfide can adsorb directly to gold to form alkanethiolates. See: Zhong, C.-J.; Porter, M. D. *J. Am. Chem. Soc.* **1994**, *116*, 11616.

(13) One could use a bis-disulfide such as H₃CSS-Ar-SSCH₃; however, there would be competition for the gold sites between the desired arylsulfide portions and the methyl sulfide portions. See: Bain, C. D.; Whitesides, G. M. *J. Am. Chem. Soc.* **1989**, *111*, 7164.

(14) Laibinis, P. E.; Whitesides, G. M.; Allara, D. L.; Tao, Y.-T.; Parikh, A. N.; Nuzzo, R. G. *J. Am. Chem. Soc.* **1991**, *113*, 7152.

(15) Parikh, A. N.; Allara, D. L. *J. Chem. Phys.* **1992**, *96*, 927.

(16) Allara, D. L.; Parikh, A. N.; Tour, J. M.; Burgin, T. P. Unpublished results.

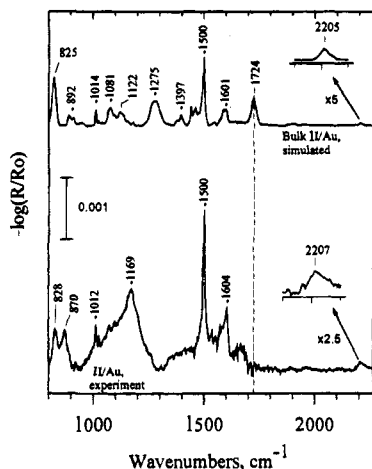


Figure 3. Simulated (top) and experimental (bottom) low wavenumber portion of the FTIR spectrum of **2** after SAM formation on Au. The apparatus and conditions were as described for Figure 2.

The simplest way to interpret these spectra is by comparison with reference spectra of a pure phase of the adsorbate molecules. The differences between the two spectra can be used to identify any perturbations of the molecular structure in the film relative to the reference state. Since both the XPS and ellipsometry data indicate that the SAM is packed at a high density, the spectrum of the bulk solid phase of **2** was used as the reference. The latter was obtained from the transmission spectra of a polycrystalline dispersion of the adsorbate compound in a pressed KBr matrix. In order to enable a quantitative comparison, the KBr pellet spectra were transformed into optical function spectra which in turn were used to simulate the reflection spectra of isotropic (randomly oriented) thin films of **2**. The film thickness was determined by ellipsometry. The simulated spectra are shown in Figures 2 and 3. The methods for the previous procedures are based on a classical electromagnetic theory approach to the description of the vibrational excitations and details can be found elsewhere.¹⁵

In general, there is close correspondence between the frequencies and line widths of the simulated and experimental spectra indicating that there is little perturbation of the chemical structure upon formation of the SAM. Figure 2 shows the C–H stretching modes. The peaks in the region of ~ 2800 to 3000 cm^{-1} are associated with the ethyl group while the high-frequency bands are associated with the aromatic protons. These latter peaks appear in approximately the same spectral region but the positions and intensities are somewhat different from the reference spectra obtained from a KBr pellet of the pure thioacetate compound (Figure 2). The changes are attributed to orientational effects in the monolayer but quantitation of these effects was not possible because of the uncertainty of correct assignments of the transition moments of the individual modes. The exact origin of the strong peak at 3067 cm^{-1} and a slightly weaker peak at ~ 3036 cm^{-1} in the monolayer spectrum (Figure 2) could not be unambiguously resolved at the present state of the work. The assignment and the estimation of the transition moment direction of the associated mode(s) are complicated by the fact that the three phenyl rings are not exactly equivalent. The replacement of a proton in the central ring by an ethyl group and the presence of –S–Au bond on the terminal ring preclude us from making accurate assignment of the peak to a specific

(17) For mode assignments in aromatic compounds, see: Varsanyi, G. *Assignments for Vibrational Spectra of Seven Hundred Benzene Derivatives*; Wiley: New York, 1974; Vol. 1. See p 14 therein for a detailed description of the a_1 mode, also termed mode 19a. The C–C vibrations in this mode involve an equal compression of the 1–2 and 6–1 ring bonds with an equal extension of the 3–4 and 4–5 bonds, where the 1 and 4 positions are located along the long molecular axis in compound **2**.

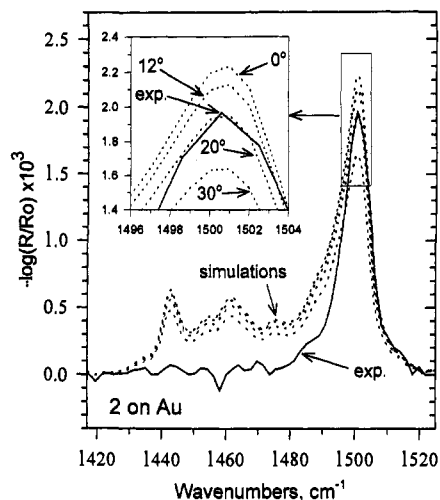


Figure 4. Comparison of the 1500-cm^{-1} region experimental spectrum of **2** after SAM formation on Au and corresponding spectra simulated for different tilt angles of the long molecular axis from the surface normal. The inset shows a magnified view of the 1500-cm^{-1} peak.

vibration. A detailed quantitative vibrational spectroscopic analysis of this peak will require examination of spectra of many analogous compounds of the same general class.¹⁶

There are a number of features in the low-frequency spectrum of **2**, but several are of particular interest (Figure 3). First, the peak at 1724 cm^{-1} in the simulated spectrum is assigned to the C=O stretching mode of the thioacetyl group in the starting compound **2**. The absence of this peak in the spectrum of the SAM is consistent with the loss of the acetyl group prior to adsorption and demonstrates that the thioacetyl group is a useful precursor for formation of thiolate monolayers. Second, the very sharp, intense peak at ~ 1500 cm^{-1} is assigned to an in-plane, C–C stretching mode of the aromatic rings.¹⁷ Although there are three different rings in **2**, they are of sufficiently similar structure that the vibrational frequencies of this mode should be nearly identical, as evidenced by the sharpness of the peak. Since the molecular symmetry of **2** can be approximated as C_{2v} , the vibration can be assigned as a_1 . Further, from the normal mode description,¹⁷ the transition dipole moment can be assumed to be along the long molecular axis. Based on a previously published method,¹⁵ a series of simulations of the 1500-cm^{-1} a_1 peak were carried out for different surface orientations of the molecule using the optical constants generated from the KBr spectra. Figure 4 shows a best fit between experiment and simulation for a 20° average tilt of the long molecular axis from the normal to the gold surface. However, if one better defines the 1500-cm^{-1} a_1 peak intensities by correcting for the contribution of the $\sim 1485\text{--}1490\text{-cm}^{-1}$ shoulder, observed to be stronger in the simulated spectra, it is clear that the tilt angle of 20° can be regarded as an upper limit since the simulated intensities will all drop. A third feature of interest in Figure 3 is the weak peak observed at ~ 2205 cm^{-1} . This feature is assigned to the C=C stretching mode with an associated direction of the transition dipole moment parallel to the bond and thus parallel to the long molecular axis. Application of the above simulation analysis to this weak mode leads to an estimate of $<20^\circ$ for the average molecular tilt angle, in general agreement with the a_1 mode analysis above.

The broad peak at ~ 1169 cm^{-1} which appears in the experimental spectrum but not the simulated one (Figure 3) is likely due to the presence of some sulfone groups in the SAM. This same oxidation product was observed in the XPS analysis (Table 1). Oxidized sulfur species generally give rise to extremely strong IR vibrations in this spectral region, and it is

estimated from the relative intensity of the 1169-cm^{-1} peak in Figure 3 that only a minor fraction of the SAM is present as sulfone.

Finally, when we attempted to use other modes in the region of $1000\text{--}1300\text{ cm}^{-1}$ to deduce the chain orientation, they were obscured by the broad sulfur oxidation feature. The two weak peaks between 1400 and 1500 cm^{-1} in the bulk simulated spectrum (Figure 3, top) can be attributed to vibrational mode 19b of the aromatic rings¹⁷ (b_2 symmetry) with the directions of the transition dipole moments aligned perpendicular to the long axis of the molecule and in the plane of the phenyl rings. Their diminution in the monolayer spectrum (Figure 3, bottom) below the noise level indicates a near-vertical orientation of the molecule, but quantitation is difficult because of the interference with the large 1500-cm^{-1} peak. Likewise, the peaks at 828 and 870 cm^{-1} are so near the detector cutoff that quite large artifacts can appear and make this region extremely unreliable.

Summary

Rigid-rod conjugated molecules with a thiol terminus can form SAMs with a high density of packing. The oligomers

need not have alkyl groups to promote the packing. The adsorption rates are slower than for alkanethiols. The use of acetyl-protected thiols is a convenient method for the in situ, based-promoted, liberation of the thiol. Moreover, the acetyl-protected thiols can adsorb directly on the gold, without the use of exogenous base. The linear dithiols tend to form SAMs in which only one thiol is attached to the surface. Oxygen-promoted multilayer formation is particularly problematic with these aromatic dithiols. These difficulties can be overcome by the direct adsorption of the α,ω -dithioacetyl compounds. This might have use in the binding of these oligomers between proximate gold probes for molecular electronics studies.

Acknowledgment. The work at all three laboratories was supported by the Advanced Research Projects Agency (ARPA). Support from the National Science Foundation (DMR-900-1270; SOA) to D.L.A. is also acknowledged. The XPS was obtained through the ARPA University Research Initiative and maintained in the Harvard Materials Research Laboratory. We thank Carl Weisbecker for assistance with the XPS.

JA950356O